A DEM investigation of the shearing behaviour of non-active clays

Arianna Gea Pagano[1,*], *Vanessa* Magnanimo[2], and *Alessandro* Tarantino[1]

[1]University of Strathclyde, Department of Civil and Environmental Engineering, Glasgow, UK
[2]University of Twente, Multiscale Mechanics Group, Enschede, Netherlands

Abstract. This paper presents the numerical DEM simulation of shear tests on two-dimensional clay-like specimens. Clay particles are modelled as rod-shaped elements made of spherical elementary units. The contact laws implemented in the adopted DEM framework account for both the mechanical interaction developing between particles in contact, and the long-range electro-chemical interaction in the form of Coulombian attraction/repulsion between charged particles. Virtual specimens for shear testing are obtained via the one-dimensional compression and unloading of clay-like particle assemblies, in order to study the effect of different over consolidation ratios on the macroscopic mechanical behaviour. The DEM framework is challenged against its ability to reproduce qualitatively key aspects of the macroscopic behaviour of normally consolidated and over consolidated clays during shearing, including contractive and dilative behaviour, and monotonic and non-monotonic stress-strain behaviour.

1 Introduction

The macroscopic behaviour of discrete materials such as soils is strongly affected by the kinematics at the micro-scale. A typical example of this is the dilative/contractive behaviour of soils upon shearing, where particle arrangements at the microscale induced by different loading histories affect the macroscopic volumetric response and the stress-strain relationship.

Microscopic mechanisms in soils may be successfully investigated using the Discrete Element Method (DEM), first proposed by Cundall and Strack [1] and widely implemented to simulate the response of granular materials (e.g. [2, 3, 4]). For the case of clayey geomaterials, DEM models may prove difficult to implement as they have to take into account both mechanical and electro-chemical interactions between particles. Also, the plate-like shape of clay particles has to be taken into account.

This paper presents the results of DEM simulations performed using a simple, two-dimensional DEM framework implemented by Pagano et al. [5, 6] using the open source C++ code MercuryDPM [7]. The DEM framework, previously validated against its ability to reproduce qualitative aspects of the one-dimensional compression of clays, was used in this study to simulate simple shear tests.

The framework was challenged to reproduce qualitatively the volumetric and mechanical macroscopic response of normally consolidated and over consolidated clays upon shearing, this corroborating its validity for the simulation of clayey geomaterials.

2 DEM analysis

2.1 DEM model

The DEM model adopted in this study is described in details in Pagano et al. [6]. Clay particles are simulated as rod-shaped particles made of spherical elementary units, bonded together via an attractive interaction. Mechanical interactions are simulated by means of conventional repulsive contact forces in the normal and tangential direction, f_{ij}^n and f_{ij}^t respectively:

$$f_{ij}^n = \begin{cases} 0, & \delta_{ij}^n \le 0 \\ k_n\delta_{ij}^n + \gamma_n v_{ij}^n, & \delta_{ij}^n > 0 \end{cases} \quad (1)$$

$$f_{ij}^t = \begin{cases} 0, & \delta_{ij}^n \le 0 \\ k_t\delta_{ij}^t + \gamma_t v_{ij}^t, & \delta_{ij}^n > 0 \\ \mu f_{ij}^n, & |k_t\delta_{ij}^t| > \mu f_{ij}^n \end{cases} \quad (2)$$

where δ_{ij} and v_{ij} are the overlap and the relative velocity between spheres i and j respectively, k is the stiffness at the contact, γ is the damping coefficient, μ is the friction coefficient, and n and t denote the normal and tangential directions respectively. The tangential contact model is extended to the rotational degree of freedom by introducing a rolling resistance, f_{ij}^{ro}, calculated by substituting the relative rotation δ_{ij}^{ro}, the rolling stiffness k_{ro}, the rolling velocity v_{ij}^{ro} , and the rolling damping coefficient γ_{ro} in Equation 2.

* Corresponding author: arianna.pagano@strath.ac.uk

Electro-chemical interactions are instead simulated by means of attractive/repulsive long-range forces in the normal direction, $f^n_{ij,Coul}$:

$$f^n_{ij,Coul} = \begin{cases} 0, & \delta^n_{ij} < \delta^{n,*}_{ij} \\ k_{Coul}(\delta^{n,*}_{ij} - \delta^n_{ij}), & \delta^{n,*}_{ij} < \delta^n_{ij} < 0 \\ k_{Coul}(\delta^{n,*}_{ij}), & \delta^n_{ij} > 0 \end{cases} \quad (3)$$

where $\delta^{n,*}_{ij}$ is the threshold particle distance corresponding to the activation of the long-range interaction for non-contacting particles, and k_{Coul} is the normal stiffness of the long-range Coulombian interaction. In order to simulate the presence of non-homogeneous surface charges on clay particles, positive or negative charges can be assigned separately to each sphere belonging to the same rod. Spheres carrying the same charge interact via repulsive long-range forces ($k_{Coul} > 0$), whereas spheres carrying opposite charges interact via attractive long-range forces ($k_{Coul} < 0$). In this study, a negative charge was assigned to the inner spheres of each rod and a positive charge to the end spheres, this resulting in edge-to-face contacts between rods. The properties assigned to the elementary spheres are shown in Table 1.

Table 1. Simulation parameters.

Input parameter	Value in SI units
Sphere density	2605 **kg/m^3**
Sphere radius	0.5e-6 **m**
Spheres per rod	19
Threshold overlap	0.5e-6 **m**
Normal stiffness	1000 **N/m**
Coulombian stiffness	0.5 **N/m**
Tangential stiffness	$2/7k_n$
Rolling stiffness	$2/5k_n$
Friction coefficient	0.3
Normal damping coefficient	5.7e-8 **kg/s**
Tangential damping coefficient	$2/7\gamma_n$
Rolling damping coefficient	$2/5\gamma_n$

2.2 DEM simulations

2.2.1 Preparation of virtual specimens

Simple-shear simulations were performed on two virtual specimens made of 300 rods, Specimen A and Specimen B. The specimens were prepared in oedometric conditions in a separate set of simulations, as described by Pagano et al. [6]. Different over consolidation ratios were obtained by choosing initial configurations prior to shearing, either belonging to the virgin compression line (OCR=1), or to an unloading-reloading line (OCR>1) in the plane $e - \sigma_z$. The loading history of Specimens A and B are shown in Figure 1. Specimen A was loaded up to a vertical stress of 2kPa (normally consolidated specimen, OCR=1). Specimen B was instead compressed up to a vertical stress of about 10kPa, and then unloaded to 2kPa (over consolidated specimen, OCR>1).

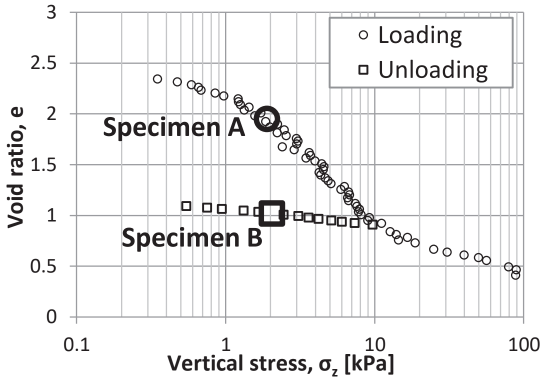

Fig. 1. Loading history of Specimen A (normally consolidated) and Specimen B (over consolidated) prior to shearing.

2.2.2 Simple shear virtual experiments

Simple shear was performed in steps by applying consecutive rotations to the left and right boundaries of the specimens. After each 10-degree rotation, the specimens were relaxed, and a vertical displacement of the top boundary was allowed in order to maintain a constant vertical stress of 2kPa.

The shear strain, shear stress and volumetric strain corresponding to each equilibrium configuration were computed in order to analyse the macroscopic behaviour of the specimens upon shearing. A schematic representation of the simulation stages is shown in Figure 2.

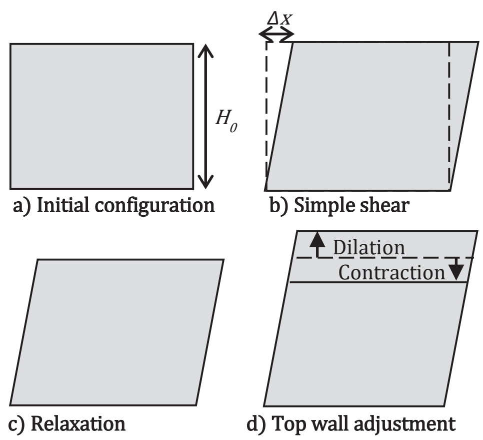

Fig. 2. Simulation stages for simple shear virtual experiments

3 Results and discussion

3.1 Volumetric macroscopic behaviour

Figure 3a shows the evolution of the volumetric strain, ε_v, against the shear strain, γ, applied to Specimen A and Specimen B. Snapshots of particle configurations representing the initial condition (γ=0) and equilibrium condition at γ=0.34 (wall rotation of 20 degrees) are compared in Figure 4 for Specimens A and B.

The two specimens exhibit a different volumetric behaviour upon shearing as a consequence of their different loading history. As expected, Specimen A exhibits a contractive behaviour, typical of a normally consolidated specimen (OCR=1). The top boundary of the specimen has to be lowered gradually upon shearing in order to keep a constant vertical stress (Figure 4a), this corresponding to a gradual reduction of the specimen's volume and, hence, a negative volumetric strain.
On the other hand, Specimen B exhibits a dilative behaviour upon shearing, typical of over consolidated soils (OCR>1). In this case, the top boundary of the specimen has to move upwards in order to guarantee a constant vertical stress of 2kPa, as shown in Figure 4b. The corresponding volumetric strain is therefore observed to be positive.

It is worth noticing that, although the qualitative dilative/contractive behaviour exhibited by the virtual specimens is in line with the expected behaviour, it was not possible to reach critical state conditions due to the presence of significant boundary effects upon further shearing. Thus, the simulations were stopped before reaching critical state conditions.

3.2 Stress-strain macroscopic behaviour

The evolution of the mobilised tangential stress, τ_{xz}, against the shear strain, γ, applied to Specimen A and Specimen B is shown in Figure 3b.

As for the volumetric response, Specimens A and B exhibit stress-strain behaviours in line with the well-known experimental observations on normally consolidated and over consolidated clays. The contractive behaviour of Specimen A, typical of normally consolidated specimens, is associated to a monotonic evolution of the mobilised tangential stress τ_{xz} upon shearing. The specimen is observed to approach the shear strength ($\tau_{xz,max}$ ≈1kPa) at γ=0.5, and the mobilised shear stress remains almost constant upon further shearing.

On the other hand, the mobilised τ_{xz} of Specimen B is observed to vary with the shear strain in a non-monotonic fashion. The specimen exhibits a peak strength $\tau_{xz,max}$ ≈1.5kPa at γ=0.5, followed by a reduction of τ_{xz} with increasing shear strain. It is expected that, in the absence of boundary effects, both specimens would reach the critical state shear strength upon further shearing.

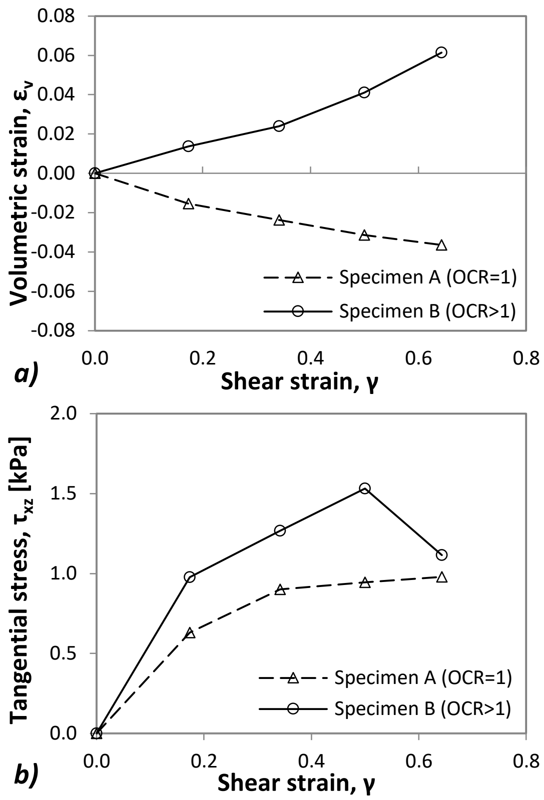

Fig. 3. *a)* Volumetric macroscopic response and *b)* mechanical behaviour of Specimen A and Specimen B upon shearing

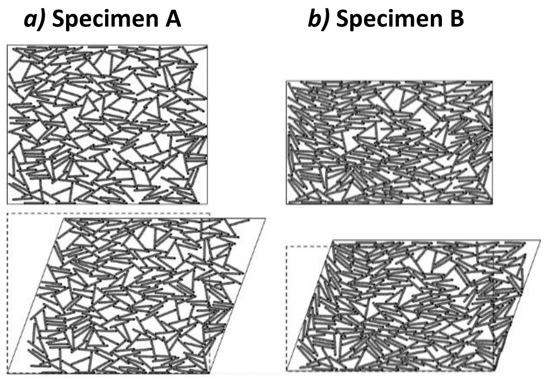

Fig. 4. Particle configuration prior to shearing (top) and after shearing to γ=0.34 (bottom) for *a)* Specimen A, and *b)* Specimen B. Dotted lines represent the size and shape of the specimens before shearing

4 Conclusions

This paper has presented the application of a simple, two-dimensional DEM framework for the simulation of clayey geomaterials, previously developed and validated by Pagano et al. [5, 6]. The DEM framework was used in this study to perform simple shear tests carried out on normally consolidated and over consolidated clay-like specimens. Clay particles were simulated as rod-shaped elements interacting via both mechanical and electro-chemical forces. Initial configurations prior to shearing were extracted from existing simulations of one-dimensional compression and unloading of clay-like specimens [6]. In particular, specimens having different over consolidation ratios were obtained by choosing initial configurations either belonging to the virgin compression line (OCR=1), or to an unloading-reloading line (OCR>1) in the plane $e - \sigma_z$.

The mechanical and volumetric macroscopic response exhibited by the virtual specimens were observed to be qualitatively in line with the widely observed behaviour of normally consolidated and over consolidated clays. Specimen A (OCR=1) was observed to contract upon shearing, and exhibited a monotonic variation of the mobilised shear stress with increasing shear strain. On the contrary, Specimen B (OCR>1) showed a dilative behaviour upon shearing, corresponding to a non-monotonic stress-strain relationship.

The ability of the DEM framework to capture the qualitative trends upon shearing is indeed extremely promising. Further numerical investigation using larger specimens or periodic boundary conditions (Lees-Edwards under simple-shear) are expected to prevent boundary effects and allow the model to capture the qualitative behaviour up to the critical state, in terms of both volumetric and mechanical behaviour.

References

1. P. A. Cundall, O. D. Strack, Geotechnique, **29**, 47-65 (1979)
2. C. O' Sullivan, J. D. Bray, L. Cui, GeoCongress 2006 (2006)
3. J. O'Donovan, C. O' Sullivan, G. Marketos, Granular Matter, **14**, 733–747 (2012)
4. T. Ueda, T. Matsushima, Y. Yamada, Granular Matter, **15**, 675–684 (2013)
5. A. G. Pagano, A. Tarantino, M. Pedrotti, V. Magnanimo, C. R. Windows-Yule, T. Weinhart, Proceedings of Powders & Grains (2017)
6. A. G. Pagano, V. Magnanimo, T. Weinhart, A. Tarantino, Geotechnique (recommended for publication, 2018)
7. T. Weinhart, D. R. Tunuguntla, M. P. van Schrojenstein-Lantman, A. J. van der Horn, I. F. C. Denissen, C. R. Windows-Yule, A. R. Thornton, Proceedings of the 7th International Conference on Discrete Element Methods, 1353-1360 (2016)